Research Paper

Plasma exosomes carrying mmu-miR-146a-5p and Notch signalling pathway–mediated synaptic activity in schizophrenia

Zhichao Wang*, MSc; Tong Wu*, PhD; Houjia Hu*, MSc; Alabed Ali A. Alabed, PhD; Guangcheng Cui, PhD; Lei Sun, MSc; Zhenghai Sun, MSc; Yuchen Wang, MSc; Ping Li, PhD

Background: Schizophrenia is characterized by a complex interplay of genetic and environmental factors, leading to alterations in various molecular pathways that may contribute to its pathogenesis. Recent studies have shown that exosomal microRNAs could play essential roles in various brain disorders; thus, we sought to explore the potential molecular mechanisms through which microRNAs in plasma exosomes are involved in schizophrenia. **Methods:** We obtained sequencing data sets (SUB12404730, SUB12422862, and SUB12421357) and transcriptome sequencing data sets (GSE111708, GSE108925, and GSE18981) from mouse models of schizophrenia using the Sequence Read Archive and the Gene Expression Omnibus databases, respectively. We performed differential expression analysis on mRNA to identify differentially expressed genes. We conducted Gene Ontology (GO) functional and Kyoto Encyclopedia of Genes and Genomes (KEGG) pathway enrichment analyses to determine differentially expressed genes. Subsequently, we determined the intersection of differentially expressed microRNAs in plasma exosomes and in prefrontal cortex tissue. We retrieved downstream target genes of mmu-miR-146a-5p from TargetScan and used Cytoscape to visualize and map the microRNA–target gene regulatory network. We conducted in vivo experiments using MK-801–induced mouse schizophrenia models and in vitro experiments using cultured mouse neurons. The role of plasma exosomal miR-146a-5p in schizophrenia was validated using a cell counting kit, detection of lactate dehydrogenase, dual-luciferase assay, quantitative reverse transcription polymerase chain reaction, and Western blot analysis. **Results:** Differential genes were mainly enriched in synaptic regulation–related functions and pathways and were associated with neuronal degeneration. We found that mmu-miR-146a-5p was highly expressed in both prefrontal cortical tissue and plasma exosomes, which may be transferred to lobe cortical vertebral neurons, leading to the synergistic dysregulation of gene network functions and, therefore, promoting schizophrenia development. We found that mmu-miR-146a-5p may inhibit the Notch signalling pathway–mediated synaptic activity of mouse pyramidal neurons in the lobe cortex by targeting *NOTCH1*, which in turn could promote the onset and development of schizophrenia in mice. **Limitations:** The study's findings are based on animal models and in vitro experiments, which may not fully replicate the complexity of human schizophrenia. **Conclusion:** Our findings suggest that mmu-miR-146a-5p in plasma-derived exosomes may play an important role in the pathogenesis of schizophrenia. Our results provide new insights into the underlying molecular mechanisms of the disease.

Introduction

Schizophrenia is a chronic psychiatric disorder that affects early brain development and is characterized by psychotic symptoms, including hallucinations, delusions, unclear thinking, and motivational and cognitive dysfunction.[1] Patients with this disorder have very high mortality.[2] Functional brain changes in schizophrenia appear in different regions of the prefrontal cortex and may eventually interact through interference between a large number of brain networks.[3–5] In particular, altered neuronal synaptic activity is one of the main cellular mechanisms leading to schizophrenia.[6] Moreover, in the cerebral cortex of patients with schizophrenia, the density of dendritic spines

Correspondence to: Guangcheng Cui and Ping Li, Department of Psychology, Qiqihar Medical University, 333 Bukui Street, Jianhua Distict, Qiqihar 161000, Heilongjiang Province, PR China; gccui@qmu.edu.cn (Cui); qyliping@qmu.edu.cn (Li)

*Share first authorship.

Submitted Aug. 14, 2023; Revised Mar. 13, 2024; Revised May 22, 2024; Accepted May 25, 2024

Cite as: *J Psychiatry Neurosci* 2024 August 29;49(4). doi: 10.1503/jpn.230118

and the average somal area of pyramidal neurons is reduced; the dysfunction of pyramidal neurons in schizophrenia may be mediated in part by a coordinated dysfunction of gene networks, which results from the altered expression of microRNAs.[7] Indeed, altered expression of microRNAs (particularly miR-146a-5p) has been reported in many neurodegenerative diseases, including Alzheimer disease, age-related macular degeneration, ataxia, dementia, multiple sclerosis, Parkinson disease, and prion disease.[8–10]

Exosomes can deliver small molecules to neurons and have an effect on cellular function.[11] Alterations in related molecules in the prefrontal cortex have been reported to possibly contribute to cognitive deficits among patients with schizophrenia.[12] Furthermore, research has found that alterations in specific molecules in the prefrontal cortex may contribute to cognitive impairments among people with schizophrenia.[13]

MicroRNAs can be detected in serum and other body fluids, serving as biomarkers for diseases. Secreted microRNAs, especially those enclosed in extracellular vesicles like exosomes, may mediate paracrine and endocrine communication between different tissues, thereby regulating gene expression and modulating cellular functions. Given the capacity of small extracellular vesicles to cross the blood–brain barrier, neuronal or glial-derived exosomes can be purified from peripheral blood and exogenous exosomes containing their cargo can be injected into the circulation to intervene in neuropsychiatric disorders.[14,15] In addition, exosomes exhibit a dual lipid membrane structure, enabling them to protect their cargo from degradation by extracellular enzymes.[16] In recent years, accumulating evidence suggests that exosomes exert considerable influence on the pathogenesis of neuropsychiatric disorders such as major depressive disorder (MDD), Alzheimer disease, and heroin addiction. For instance, researchers injected plasma from patients with MDD into healthy mice and found that it induced depressive-like behaviour, while injecting plasma from controls reduced depressive-like behaviour in a depressive mouse model.[17] Another study identified alterations in exosomal microRNAs (miR-21–5p, miR-30d-5p, miR-486) associated with MDD.[18] Dysregulation of secreted microRNAs can lead to tissue dysfunction, aging, and disease. Adipose tissue is an important source of circulating exosomal microRNAs.[19] Reports have suggested that exosomes can exert functional effects on neurons by delivering small molecules into them.[20,21] Levels of factors in plasma have been implicated in schizophrenia,[22] but the effect of microRNAs in plasma exosomes on schizophrenia remains unclear.

The Notch signalling pathway is recognized as a major regulator of neural stem cells and neural development; it is involved in coordinating neurogenesis, axon growth, synapse formation, and induction of neuronal apoptosis in the adult brain to facilitate neural system development and patterning.[23] These findings have positioned it as a suitable candidate to explore psychotic disorders. The association between the Notch signalling pathway and schizophrenia was initially discovered through genetic studies that linked the *NOTCH4* gene to schizophrenia among trios of British parents and offspring,[24] which was later confirmed by larger-scale genome-wide association studies.[25] Aside from its crucial role in regulating neural cell proliferation, differentiation, and neurite outgrowth, the Notch signalling pathway also acts as a key factor in adaptive and innate immune responses.[26] Notch and its ligands, such as δ-like protein 1 (DLL1), are implicated in endothelial dysfunction and vascular inflammation,[27,28] as well as macrophage activation;[29] they participate in the crosstalk between immune cells and the brain during ischemic stroke. This may also be relevant to severe psychotic disorders as schizophrenia involves immune-mediated pathogenic mechanisms, highlighting the crucial role of investigating the relationship between schizophrenia and the Notch pathway to unravel schizophrenia's pathogenesis.[30] To gain a better understanding of the mechanisms underlying schizophrenia and to identify potential molecular targets for treatment, we conducted an analysis using a combination of schizophrenia-related microarray data sets of mice and schizophrenia-related sequencing data sets. The aim was to explore the potential molecular mechanisms through which microRNAs in plasma exosomes are involved in schizophrenia.

Methods

Data download

We downloaded the sequencing data sets related to mouse models of schizophrenia from the Sequence Read Archive (SRA) database (https://www.ncbi.nlm.nih.gov/sra/), namely SUB12404730, SUB12422862, and SUB12421357. The mice in the treatment groups of these 3 data sets were successfully induced with schizophrenia by administration of MK-801. Specifically, SUB12404730 consists of transcriptome sequencing data from the prefrontal cortex tissue of mice with schizophrenia (6 mice in the control group and 6 mice in the treatment group); SUB12422862 contains microRNA sequencing data from plasma exosomes of mice with schizophrenia (6 mice in the control group and 6 mice in the treatment group). Lastly, SUB12421357 encompasses microRNA sequencing data from the prefrontal cortex tissue of mice with schizophrenia (9 mice in the control group and 10 mice in the treatment group).

We obtained the transcriptome sequencing data sets related to mouse models of schizophrenia (GSE111708, GSE108925, and GSE18982) from the Gene Expression Omnibus (GEO) database (http://www.ncbi.nlm.nih.gov/geo/). In the GSE111708 data set, tissue samples from the prefrontal cortex were collected from 3 control mice and 6 mice with schizophrenia, induced using MK-801 treatment. The GSE108925 data set includes tissue samples from the prefrontal cortex of 6 control mice and 6 mice with schizophrenia, induced using methylazoxymethanol treatment. Finally, the GSE189821 data set consists of tissue samples from the prefrontal cortex of 12 control mice and 12 mice with schizophrenia, induced using Δ-9-tetrahydrocannabinol treatment. All data sets

are in fragment per kilobase million (FPKM) format. The chip annotation information was sourced from the GENCODE database (https://www.gencodegenes.org/human/). We used Perl programming language to merge the 3 chip data sets, and the sva combat package (www.bioconductor.org/help/search/index.html?q=sva/) for batch correction of the samples. After merging, the total data set included 21 prefrontal cortex samples from control mice and 24 prefrontal cortex samples from mice with schizophrenia.[31]

Screening for differentially expressed genes

We used the limma package of R software (https://bioconductor.org/packages/limma/) to analyze the data set for differential gene expression. We used the false discovery rate (FDR) method to correct the differential p values (FDR < 0.05 and log fold change > 1 were thresholds to determine significantly differentially expressed genes). We used the pheatmap package (www.bioconductor.org/help/search/index.html?q=pheatmap/) and the ggplot2 package (http://www.bioconductor.org/help/search/index.html?q=ggplot2/) to plot the heat map and volcano map, respectively. We compared data between the 2 groups using the Wilcoxon rank sum test (wilcox.test package). All analyses in this paper were performed using R version 4.2.1.

Enrichment analysis

We analyzed differential genes with Gene Ontology (GO) and Kyoto Encyclopedia of Genes and Genomes (KEGG) enrichment analysis using the ClusterProfiler package in R (https://www.bioconductor.org/packages/release/bioc/html/clusterProfiler.html). There are 3 levels of GO enrichment analysis, namely biological process, cellular component, and molecular function (threshold of $p < 0.05$ for selection). We performed KEGG enrichment analysis to identify significantly enriched cellular functions and signalling pathways for differential genes (threshold of $p < 0.05$ for selection).

Constructing microRNA–target gene regulatory networks

We retrieved the mmu-miR-146a-5p (from *Mus musculus* [mmu]) downstream target genes from the TargetScan database (www.targetscan.org/) and intersected these with differentially expressed mRNAs to obtain microRNA–target gene pairs. We used Cytoscape software (version 3.6.0) for visualization and mapping of the microRNA–target gene regulatory network.

Animal experiments

Six-week-old and newborn C57BL/6J mice, provided by the Laboratory Animal Center of Qiqihar Medical University (license no. SYXK(Hei)2021–013), were fed in nonpathogenic conditions at 26–28°C and 50%–65% humidity. They had free access to food and water, with a 12-hour light and dark cycle.

We randomly divided mice into control and schizophrenia groups. They were adaptive fed for 7 days and underwent drug injections on the eigth day. The schizophrenia group received intraperitoneal injections of MK-801 (M107, Sigma-Aldrich) twice a day (at 9:00 and 16:00). Before each injection, the mice were weighed and injected with MK-801 at a concentration of 0.5 mg/kg. The exact volume of the MK-801 injection was determined based on the weight of each mouse. The control group received injections of physiologic saline. This injection protocol was carried out consecutively for 6 days.[32]

Morris water maze test

We used the Morris water maze test to assess the learning and memory function of the mice in each group. The experiment took place in a circular, black-painted swimming pool measuring 150 cm in diameter and 50 cm in depth. The pool was filled with clear water at a depth of about 30 cm, and nontoxic black ink was added to make the water appear black. The surface of the water was divided into 4 quadrants, with a platform (diameter of 10 cm) positioned in the centre of 1 of the quadrants. The platform was situated about 2 cm below the water surface. The experiments began at 9:00 each day, with the water temperature maintained at 24° (± 1°) C. Before the test, we conducted a place navigation task, wherein 1 of the 4 quadrants (each quadrant having a fixed release point) was selected randomly for placing the mice, facing the wall of the pool. We recorded the time taken for the mice to locate the platform in the water and the duration of their stay on the platform. If a mouse failed to find the platform within 60 seconds, it was guided to the platform and allowed to stay there for 30 seconds. We considered the time taken to locate the platform as the escape latency, reflecting the learning ability of mice. If a mouse failed to find the platform within 60 seconds, the time was recorded as 60 seconds. After moving the animals away from the pool, they were dried and the next experiment was conducted after an interval of 10–15 minutes. We conducted 4 experiments each day for 4 consecutive days. On the fifth day, we performed a spatial probe trial by removing the platform from the water. The mice were placed in the water with their backs toward the pool at the location where the platform was previously positioned. We recorded the time spent by the mice in the quadrant where the platform was originally placed and the number of times they crossed the original platform as the memory retention period.[33]

Measurement of pre-pulse inhibition

The measurement of pre-pulse inhibition (PPI) is a sensorymotor gating operation that provides information about the extent to which information processing absorbed by the prepulse is interrupted by subsequent startling stimuli. Before testing, mice were habituated for 30 minutes. We assessed PPI using the SR-LAB Startle Response System (San Diego Instruments) by presenting pre-pulse stimuli at 4, 8, and 16 dB

above a background noise level of 65 dB to evaluate the suppression of startle response caused by a startling pulse stimulus of 120 dB. To assess PPI, we calculated a percentage score as follows: PPI = 100 × ([startle response to single pulse stimulus – (pre-pulse + pulse stimulus)] / startle response to single pulse stimulus).[33]

Extraction of plasma exosomes

We obtained whole-blood samples from mice in the schizophrenia and control groups using a venipuncture needle and ethylenediaminetetraacetic acid anticoagulant tubes, gently mixed at room temperature. After centrifugation at 1900 *g* at 4°C for 10 minutes, we obtained plasma from the supernatant. The plasma was centrifuged at 4°C for 15 minutes at 3000 *g*, 10 minutes at 500 *g*, 20 minutes at 20 000 *g*, and 70 minutes at 10 000 *g*. Exosomes were deposited at the bottom of the centrifuge tube. We removed the supernatant, washed the sample with phosphate-buffered saline (PBS), and centrifuged it again at 10 000 *g* for 70 minutes. Plasma exosomes precipitated at the bottom of the centrifuge tube, and we added 20 µL of PBS to resuspend exosomes for follow-up experiments.[34]

Identification of plasma exosomes

We observed morphological characteristics and the distribution of particle size of exosomes using transmission electron microscopy and a nanoparticle tracer analyzer, respectively.

We diluted plasma exosomes to an optimal concentration (1 mg/mL), placed in Formvar membrane copper mesh (size 300), and fixed under infrared lamp for 30 minutes. The samples that were not attached to the copper net were carefully absorbed with filter paper, and then the remaining sample was placed in 2.5% glutaraldehyde phosphate buffer (G5882, Sigma-Aldrich) for 15 minutes, then washed twice with PBS and distilled water. We used phosphotungstate suspension drops (P4006, Sigma-Aldrich) for negative staining, viewed under transmission electron microscope.

The nanoparticles in the liquid have random Brownian motion from the impact of the surrounding solution molecules. We analyzed plasma exosomes by nanoparticle tracer analyzer. We diluted the mouse plasma exosomes, obtained after ultracentrifugation, to the appropriate concentration, and the appropriate amount was added to the nanoparticle tracer analyzer (ZetaView PMX-110, Particle Metrix). We recorded the particle movement trajectory under the appropriate background and determined the distribution diagram of the sample concentration and particle diameter. We obtained the exosome concentration according to the dilution ratio.[35]

Cultivation of isolated cone-shaped neurons in the mouse cerebral cortex

The newborn mice were wiped with 75% alcohol and decapitated. We quickly removed the brains and placed them in a dish containing pre-cooled Hanks' Balanced Salt Solution (H6648, Sigma-Aldrich). The cortex was separated, the dura mater and blood vessels were removed with ophthalmic tweezers, and the cortex was cut to a tissue block with a diameter of about 1 mm. This process allowed for the careful isolation of cortical neurons. We placed the tissue blocks into 5-mL centrifuge tubes containing 0.125% pancreatic enzyme (T4799, Sigma-Aldrich), digested in a 37°C water bath for 17 minutes, and then digested with 0.5 mL 1% DNase (10104159001, Sigma-Aldrich) for 5 minutes at room temperature. The enzyme solution was slowly aspirated, and Hanks' Balanced Salt Solution was added to dilute any residual enzyme solution. After 5–7 repetitions of this washing process, we added Dulbecco's Modified Eagle Medium/Nutrient Mixture F-12 (DMEM/F-12) medium (D9785, Sigma-Aldrich). The tissue blocks were then gently triturated with a pipette around 20 times until a single-cell suspension was achieved.

We counted cells using a hemocytometer and determined the number of neurons (per mL). Based on the cell count, we plated the neurons onto 96- or 6-well plates, as required for the experimental setup. After a 4-hour attachment period, we replaced the DMEM/F-12 medium with Neurobasal medium (SCM003, Sigma-Aldrich). We used these cultured neurons in subsequent experiments, with each experiment replicated at least 3 independent times.[36]

Exosome uptake in vitro

We stained exosomes using the PKH67 green fluorescent labelling kit (PKH67GL, Sigma-Aldrich). We added 6 µL of exosome solution to 244 µL of dilution buffer C and mixed well. We then added 1 µL of PKH67 to 249 µL of dilution buffer C in a centrifuge tube and mixed thoroughly. The exosome suspension (250 µL) was immediately added to 250 µL of PKH67 dye, and the sample was quickly and uniformly mixed using a pipette. The mixture was incubated at 25°C for 4 minutes with gentle inversion of the centrifuge tube. To stop the staining, we added 1% bovine serum albumin (V900933, Sigma-Aldrich). After staining, we added 6 mL of PBS, and exosomes were separated again using high-speed centrifugation, as previously described. After centrifugation, we resuspended the exosomes in 200 µL of DMEM/F-12 complete culture medium. The exosomes labelled with PKH67 (200 µg/mL) were co-cultured with isolated cortical cone-shaped neurons[37] at 37°C for 12 hours under light-protected conditions. Subsequently, the samples were rinsed 3 times with PBS, fixed with 4% paraformaldehyde (P6148, Sigma-Aldrich) for 20–30 minutes, and then rinsed with PBS 3 times. Nuclei were stained with 4',6-diamidino-2-phenylindole (D9542, Sigma-Aldrich) for 5 minutes. We observed fluorescence distribution under a fluorescence microscope, followed by quantitative analysis.[35]

Cell transfection

We transfected the recombinant lentivirus plasmid — carrying miR-NC (negative control) inhibitor or miR-146a-5p inhibitor, as well as miR-NC mimic or miR-146a-5p mimic (Appendix 1, Table S1, available at www.jpn.ca/lookup/doi/10.1503/jpn.230118/tab-related-content) — into 293T

cells using Lipofectamine 2000 reagent (11668019, Thermo Fisher Scientific). After about 48 hours, we collected the supernatant containing the virus, filtered it through a 0.45-μm cellulose mixed filter, and stored at –80°C for subsequent experiments. Primary cortical pyramidal neurons were infected with the lentiviral vectors at an appropriate infection multiplicity and cultured for an additional 24 hours before harvesting the cells for further analysis. We purchased all lentiviruses from Shanghai Genomic Engineering Biotechnology; primer sequences and plasmid constructs were provided by the same company. We conducted the experimental procedures in accordance with the manufacturer's instructions. After 48 hours of viral infection, neurons were co-cultured with exosomes (following the same method as described previously) for subsequent experiments. The experiments were repeated 3 times.[35]

Cell counting assay

The measured neurons were prepared into single-cell suspension and inoculated into 96-well plates, with about 3000–4000 cells per well. After 72 hours of cell culture, we used the Cell Counting Kit-8 (CCK-8; 96992, Sigma-Aldrich) with one-tenth of the total volume added, according to the practical instructions, and incubated for 4 hours under CO_2. For each well, we measured the absorbance value at 450 nm by microplate reader, and calculated the cell activity as follows: cell activity (%) = (absorbance value$_{treatment}$ – absorbance value$_{blank}$)/(absorbance value$_{control}$ – absorbance value$_{blank}$).[38]

Detection of lactate dehydrogenase release

Lactate dehydrogenase (LDH) release is commonly used as an indicator to assess cell toxicity or damage. To establish a cell suspension of the neurons under investigation, they were cultured as single cells in a 96-well plate, with about 3000–4000 cells per well. After 72 hours of cell culture, we took the cell culture plate out 1 hour before detection. We added LDH-releasing reagent (11644793001, Sigma-Aldrich) into the control well to determine maximum enzyme activity of sample, which was 10% of the volume of the culture medium, triturated, and cultured again. During the test, 60 μL of supernatant was taken and transferred to another 96-well plate. We added 30 μL of the LDH detection working liquid into each well and mixed evenly. We detected the absorption value at 490 nm of each well by microplate reader and calculated LDH release as follows: LDH release = (absorbency value$_{treatment}$ – absorbency value$_{control}$)/(absorbency value$_{maximum\ enzyme\ activity}$ – absorbency value$_{control}$) × standard sample concentration (mU/mL).[38]

Dual-luciferase reporter gene assay

We cloned wild-type and mutant *NOTCH1* (*NOTCH1*-WT and *NOTCH1*-MUT) sequences into the pRL-TK reporter plasmid (E2241, Promega Corporation). We cultured 293T cells (CRL-3216, ATCC, https://www.atcc.org) in 96-well plates, with a density of 5000 cells per well, in DMEM-containing 10% fetal bovine serum for 24 hours. After 24 hours, the plasmid and vector were co-transfected with miR-146a-5p mimic or miR-NC mimic using Lipofectamine 2000. After 48 hours, we detected luciferase activity using a dual-luciferase reporter assay system (E1910, Promega Corporation).[39] We obtained the miR-146a-5p mimic and miR-NC mimic from Hanbio Therapeutics.

Western blot analysis

The samples were digested in RIPA lysis buffer (P0013B, Beyotime Biotechnology). We determined protein concentration using a bicinchoninic acid assay (A53226, Thermo Fisher Scientific). After protein separation by polyacrylamide gel electrophoresis, the protein was transferred to polyvinylidene fluoride membrane (IPVH85R, Sigma-Aldrich) by the wet-transfer method. The membrane was sealed in 5% bovine serum albumin at room temperature for 1 hour, and then incubated with rabbit anti-CD63 (ab217345, 1:1000, Abcam), TSG101 (ab125011, 1:1000, Abcam), calnexin (ab22595, 1:1000, Abcam), or glyceraldehyde 3-phosphate dehydrogenase (ab9485, 1:1000, Abcam, internal reference) overnight at 4°C. After washing, horseradish peroxidase–labelled secondary antibody (ab6721, 1:5000, Abcam) was added for incubation for 2 hours. We performed protein quantitative analysis using ImageJ (version 1.48).[40]

Quantitative reverse transcription polymerase chain reaction

We used TRIzol reagent (15596026, Thermo Fisher Scientific) to extract total RNA from cells or exosomes. We used the NanoDrop 2000 microultraviolet spectrophotometer (ND-2000, Thermo Fisher Scientific) to detect the concentration and purity of total RNA extracted. We reversely transcribed mRNA and long non-coding RNA into amplify DNA (PrimeScript reverse transcription [RT] reagent kit; RR047A, Takara Bio). We performed RT of microRNA using the M-MLV reverse transcription method (M1701, Promega Corporation).

We performed RT quantitative polymerase chain reaction (RT-qPCR) on the synthesized amplify DNA with the Fast SYBR Green PCR kit (11736059, Thermo Fisher Scientific), and 3 replicates were set for each well. We used glyceraldehyde 3-phosphate dehydrogenase as the reference gene of mRNA and long non-coding RNA, and U6 as the reference gene of microRNA. The $2^{-\Delta\Delta CT}$ method was used for gene expression analysis. The primer sequence is shown in Appendix 1, Table S2.

Statistical analysis

We processed data using SPSS (version 24.0) and tested all data for normal distribution and uniformity of variance. We expressed measurement data conforming to normal distribution in the form of means and standard deviations. We compared groups using independent-sample *t* tests. We considered *p* values of less than 0.05 to be statistically significant.

Ethics approval

All animal experiments were approved by the Animal Ethics Committee of Qiqihar Medical University (QMU-AECC-2020–68).

Results

Schizophrenia-associated genes and synaptic regulatory functions

The differential analysis of the whole-transcriptome sequencing data set found 1549 differentially expressed genes in prefrontal cortical tissue of control mice and mice with schizophrenia (Figure 1 and Appendix 2, Figure S1, available at www.jpn.ca/lookup/doi/10.1503/jpn.230118/tab-related-content). We performed GO and KEGG enrichment analyses on the differential genes to explore their major enrichment functions and pathways in schizophrenia. The GO functional enrichment analysis revealed that these genes were mainly concentrated in axonogenesis, negative regulation of the cell cycle, and regulation of chromosome organization in biological processes (Figure 2A). For cell components, the genes were mainly concentrated in the specialization of the actin cytoskeleton, postsynaptic specialization, and neuron-to-neuron synapses. In terms of molecular function, the genes were mainly concentrated in the activity of ATPase and enzyme activator. The KEGG pathway enrichment analysis revealed these genes were mainly enriched in the relaxin signalling pathway, cortisol synthesis and secretion, RNA polymerase, and glutamatergic synapse–related pathways (Figure 2B).

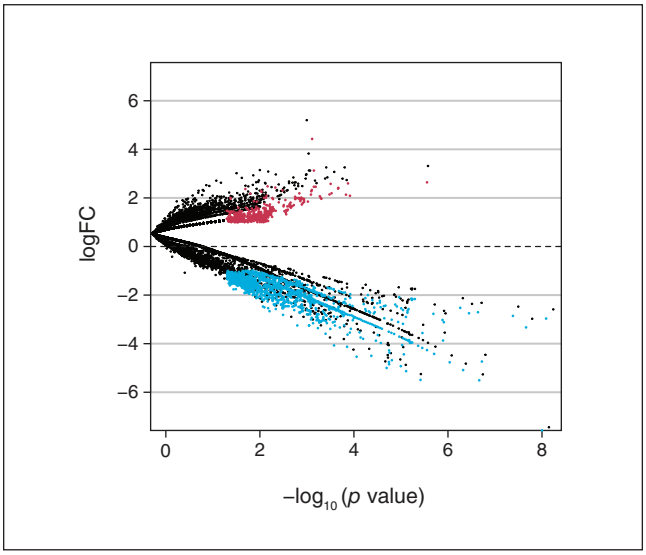

Figure 1: Volcano plot of differentially expressed genes in prefrontal cortical tissue from 6 mice with schizophrenia and 6 control mice, where each dot in the plot represents a gene. Red indicates a significantly highly expressed gene, blue indicates a significantly lowly expressed gene, and black indicates a non-differential gene. FC = fold change.

In summary, schizophrenia-related genes were mainly enriched in synaptic regulation–related functions and pathways. The occurrence of schizophrenia may be related to the synaptic activity of lobe cortical pyramidal neurons.

Schizophrenia-related genes associated with neuronal degeneration

To further investigate the pathogenic mechanism of schizophrenia, we expanded the sample size with GEO microarray data (GSE111708, GSE108925, and GSE189821). We combined and batch-corrected the microarray data and subjected the integrated data to differential analysis to obtain a total of 60 differential genes (Appendix 3, Figure S2, available at www.jpn.ca/lookup/doi/10.1503/jpn.230118/tab-related-content). Further KEGG enrichment analysis of the differential genes revealed these genes were mainly enriched in oxidative phosphorylation, Alzheimer disease, and pathways of neurodegeneration (multiple diseases) (Figure 3). Therefore, we speculated that the pathogenesis of schizophrenia may be through some molecular regulatory mechanism that affects the altered expression of disease-related genes, which in turn leads to neuronal degeneration, affects neuronal synaptic activity, and, ultimately, promotes the development of the disease.

Plasma exosomes and transmission of mmu-miR-146a-5p to pyramidal neurons in the lobe cortex

We performed a differential analysis of microRNA sequencing data in prefrontal cortex tissue and plasma-derived exosomes of mice with schizophrenia in the SRA database. We found a total of 164 differentially expressed microRNAs in prefrontal cortex tissue and 5 differentially expressed microRNAs in plasma exosomes (Appendix 4, Figure S3A and S3B, available at www.jpn.ca/lookup/doi/10.1503/jpn.230118/tab-related-content). After intersecting the 2 sets of results, the target microRNA was identified as mmu-miR-146a-5p (Figure 4A). The microRNA sequencing data showed that mmu-miR-146a-5p was highly expressed in both prefrontal cortex tissue ($t_{10} = 10.92$, $p < 0.0001$; Figure 4B) and plasma-derived exosomes ($t_{10} = 9.310$, $p < 0.0001$; Figure 4C).

Prediction of mmu-miR-146a-5p downstream target genes and construction of mmu-miR-146a-5p–target gene regulatory network

We searched the TargetScan database for possible downstream targets regulated by mmu-miR-146a-5p and obtained a total of 161 target genes. These target genes were then compared with the differentially expressed genes in the prefrontal cortex of mice with schizophrenia. The analysis revealed that 11 of the target genes displayed low expression levels in the prefrontal cortex of mice with schizophrenia (Figure 4B and Figure 5A). We visualized the microRNA–target gene regulatory network by Cytoscape (Figure 6). Thus, mmu-miR-146a-5p may be involved in the schizophrenia process by regulating these 11 differentially expressed target genes.

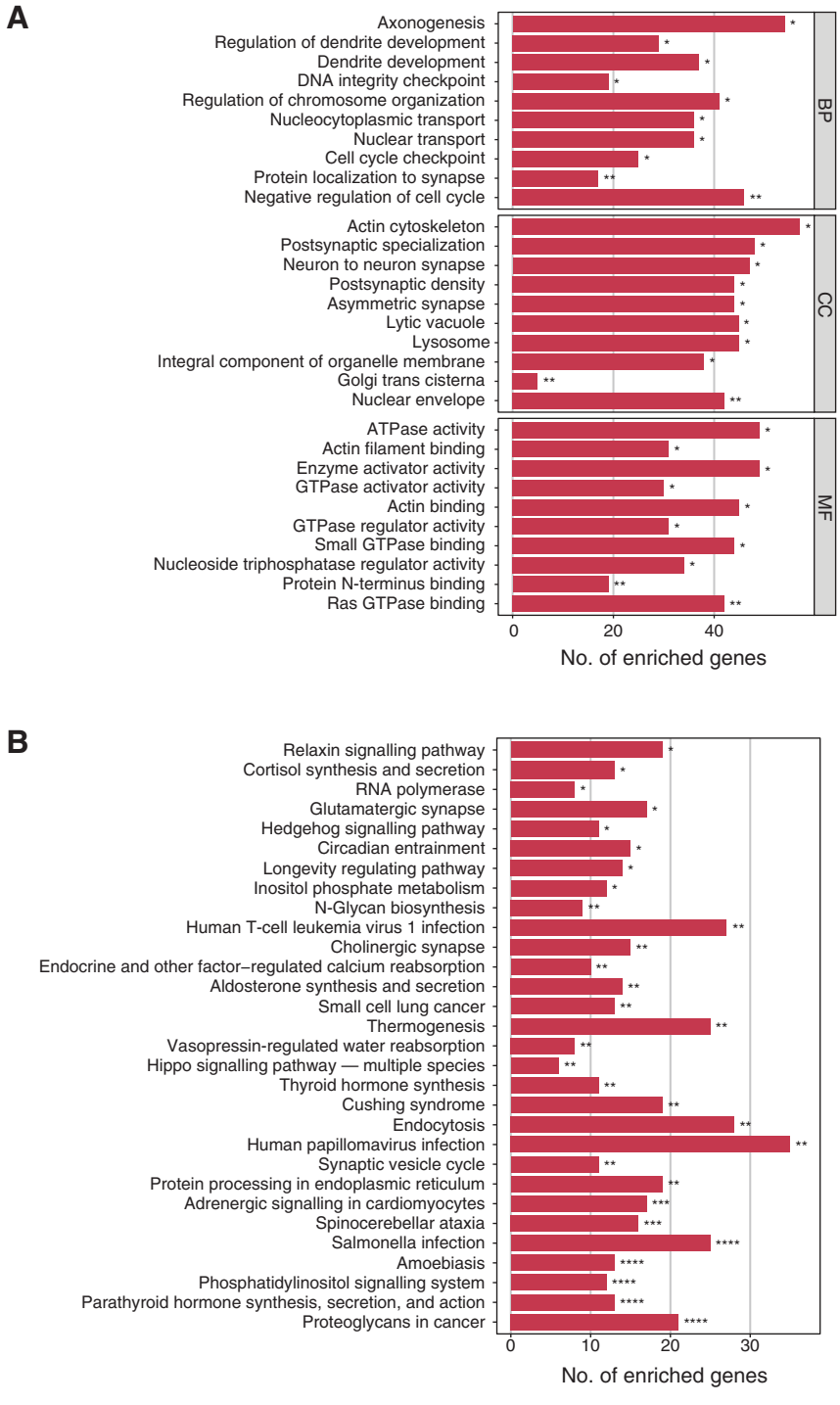

Figure 2: (A) Differentially expressed genes in Gene Ontology (GO) enrichment analysis (identified with GO name), indicating number of enriched genes and significance of difference between mice with schizophrenia and controls. (B) Differentially expressed genes in Kyoto Encyclopedia of Genes and Genomes (KEGG) enrichment analysis (identified with KEGG name), indicating number of enriched genes and significance of difference between mice with schizophrenia and controls. See Related Content tab for accessible version. BP = biological process, CC = cellular component, MF = molecular function. *$p < 0.00005$; **$p < 0.0001$; ***$p < 0.00015$; ****$p < 0.0002$.

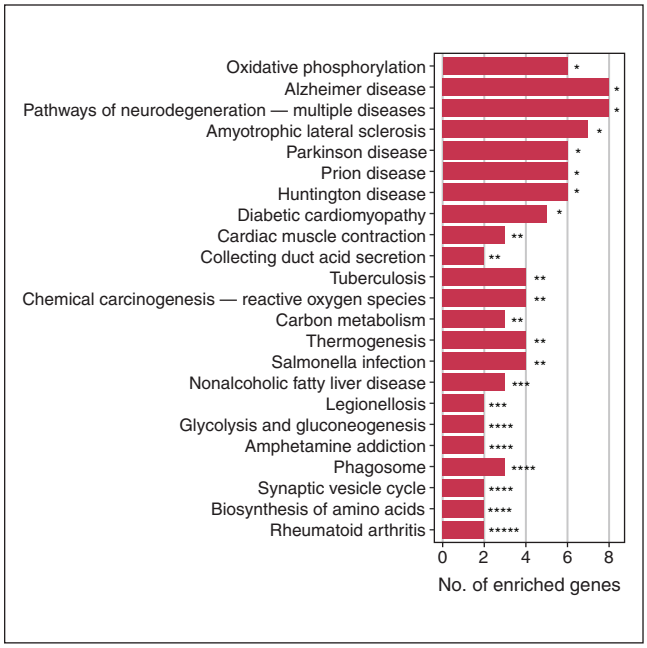

Figure 3: Differentially expressed genes in Kyoto Encyclopedia of Genes and Genomes (KEGG) enrichment analysis (identified with KEGG name), indicating number of enriched genes and significance of difference between mice with schizophrenia and controls. See Related Content tab for accessible version. *$p < 0.01$; **$p < 0.02$; ***$p < 0.03$; ****$p < 0.04$; *****$p < 0.05$.

Inhibition of Notch signalling pathway-mediated excitability activity by mmu-miR-146a-5p

We performed GO and KEGG enrichment analysis on 11 target genes of mmu-miR-146a-5p to explore their main enriched functions and pathways in schizophrenia. The results of GO functional enrichment analysis showed that these genes were mainly enriched in the entries of axonogenesis, dendrite development, dendrite morphogenesis, and axon guidance in biological processes, and in the glutamatergic synapse in the cellular component (Figure 7A). The results of the KEGG pathway enrichment analysis revealed that these genes are primarily enriched in the Notch signalling pathway (Figure 7B). Notably, *NOTCH1* exhibited the largest change, suggesting that mmu-miR-146a-5p may modulate synaptic activity in the pyramidal neurons of the mouse prefrontal cortex through the regulation of the Notch signalling pathway. Consequently, this dysregulation may contribute to the onset and progression of schizophrenia in mice.

Plasma exosomal miR-146a-5p and cortical pyramidal neuron activity

To investigate the involvement of plasma exosome mmu-miR-146a-5p in the pathogenesis and development of schizophrenia through its effect on synaptic activity in the pyramidal neurons of the prefrontal cortex, we established an MK-801–induced mouse model of schizophrenia and validated it using the Morris water maze test and PPI test. We included 12 mice, randomly divided into control and schizophrenia groups. The Morris water maze test revealed that, compared with the control group, mice in the schizophrenia group showed impaired cognitive function, characterized by increased escape latency ($t_{10} = 14.69$, $p < 0.0001$; Figure 8A), reduced number of crossings over the former platform ($t_{10} = 9.522$, $p < 0.0001$; Figure 8B), and shorter time spent in the target quadrant ($t_{10} = 12.65$, $p < 0.0001$; Figure 8C). The results of the PPI test showed significantly lower response inhibition among mice with schizophrenia at 4 dB ($t_{10} = 16.70$, $p < 0.0001$) and 8 dB ($t_{10} = 11.27$, $p < 0.0001$), compared with the control group (Figure 8D). These findings collectively confirm the construction of the mouse model of schizophrenia.

Next, we carried out the extraction and identification of plasma exosomes from mice. The Western blot analysis revealed positive expression of exosomal markers CD63 and TSG101, while calnexin exhibited negative expression (Figure 9A), indicating that exosome extraction was successful and purification reached the standard. Morphological characteristics of exosomes were observed by transmission electron microscopy. We found a small number of membrane vesicles with shallow electron density and a diameter of about 50–100 nm; some vesicles with central depression were observed, which was consistent with typical saucer-like morphological characteristics of exosomes (Figure 9B). Results from the nanoparticle tracer analyzer showed that the vesicles contained in the sample were mainly about 151.6 nm, which was consistent with the size range of exosomes (70–200 nm), further confirming that the extracted vesicles were exosomes (Figure 9C).

We conducted an in vitro uptake experiment to observe whether plasma exosomes could be absorbed by cortical neurons from 5 newborn mice. Fluorescence microscopy results showed that, after a 12-hour incubation period, green fluorescence was observed in the cytoplasm of cortical neurons incubated with PKH67-labelled exosomes, with no residual dye fluorescence in neurons with only PKH67 staining (Figure 9D), indicating that plasma exosomes could be taken up by cortical neurons.

We used RT-qPCR to measure the expression levels of miR-146a-5p in plasma-derived exosomes. The results revealed a significant upregulation of miR-146a-5p in the exosomes of mice with schizophrenia ($t_{10} = 8.599$, $p < 0.0001$; Figure 10A). After co-culture of exosomes and cortical neurons, RT-qPCR showed that the expression of miR-146a-5p in neurons was significantly higher among mice with schizophrenia than controls ($t_{10} = 11.42$, $p < 0.0001$; Figure 10B). Both the CCK-8 assay and LDH assay suggested that the neuronal activity of mice with schizophrenia was significantly lower than controls; cell damage was aggravated ($t_{10} = 9.959$, $p < 0.0001$; Figure 10C) and LDH release was increased among those with schizophrenia ($t_{10} = 6.992$, $p < 0.0001$; Figure 10D). Exosomes derived from mice with schizophrenia can transmit miR-146a-5p to pyramidal neurons in the prefrontal cortex and influence their activity.

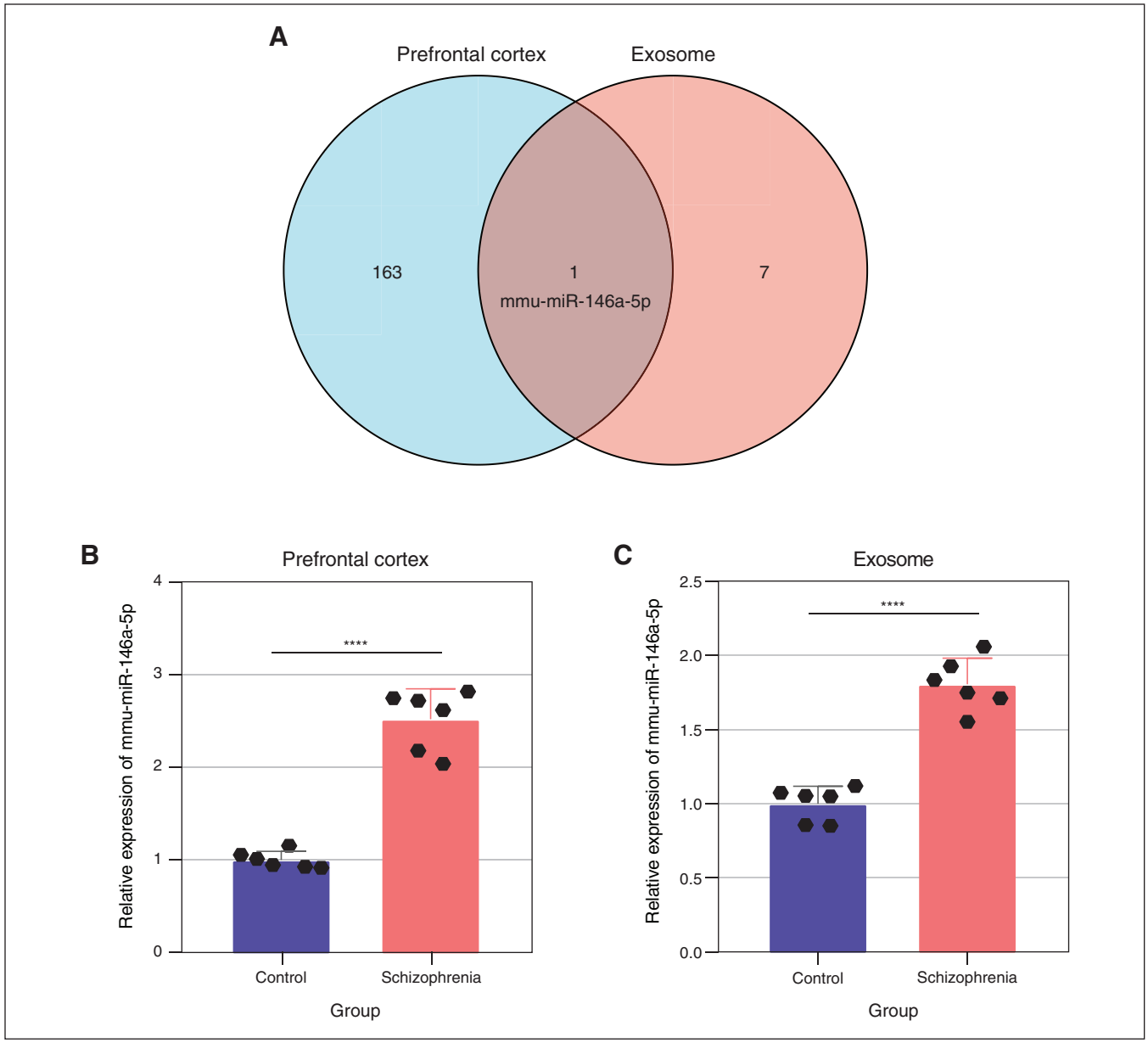

Figure 4: Expression levels of mmu-miR-146a-5p in plasma exosomes and prefrontal cortex tissues of schizophrenia mice models. (A) Wayne diagram indicating the intersection of differentially expressed microRNA in prefrontal cortex tissue (blue) and plasma exosomes (pink) of mice with schizophrenia. (B) Expression levels of mmu-miR-146a-5p in prefrontal cortical tissues and (C) plasma exosomes of 6 mice with schizophrenia and 6 control mice. See Related Content tab for accessible version. ****$p < 0.0001$.

Extracellular vesicle miR-146a-5p, functionality of pyramidal neurons in the mouse neocortex, and modulation of NOTCH1 *expression*

We used RT-qPCR to further investigate the impact of miR-146a-5p on neuronal synaptic activity via the inhibition of *NOTCH1*. The results demonstrated a significant decrease in *NOTCH1* expression in both the prefrontal cortex tissue ($t_{10} = 10.01$, $p < 0.0001$; Figure 11A) and neurons ($t_{10} = 7.544$, $p < 0.0001$; Figure 11B) of the schizophrenia group, compared with the control group. The interaction between miR-146a-5p and *NOTCH1*-WT or *NOTCH1*-MUT was further verified by dual-luciferase reporter gene assay. The binding sites of miR-146a-5p and *NOTCH1*-WT or *NOTCH1*-MUT predicted by TargetScan database are shown in Figure 11C. Co-transfection of miR-146a-5p and *NOTCH1*-WT or *NOTCH1*-MUT into 293T cells showed that the miR-146a-5p mimic significantly reduced the luciferase activity of *NOTCH1*-WT in 293T cells, compared with miR-NC mimic ($t_8 = 6.756$, $p < 0.0001$; Figure 11D). The results indicated that miR-146a-5p could target and inhibit the *NOTCH1* gene.

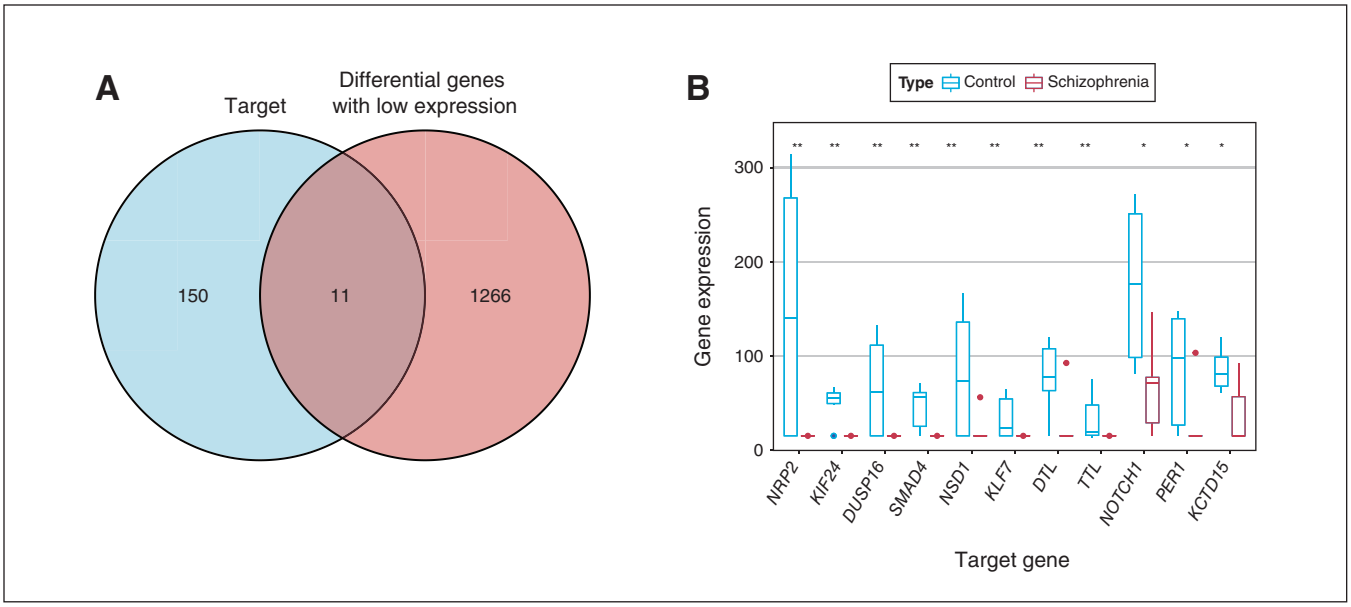

Figure 5: (A) Venn diagram indicating the intersection of mmu-miR-146a-5p target genes (blue) and differential genes with low expression in prefrontal cortex tissue (pink) of mice with schizophrenia. (B) Transcriptome sequencing data showing 11 target genes in prefrontal cortex tissue of mice with schizophrenia. See Related Content tab for accessible version. *$p < 0.05$; **$p < 0.01$.

Subsequently, we assessed mmu-miR-146a-5p expression and neuronal activity by co-cultivating neurons with plasma exosomes derived from the blood of mice with schizophrenia for 24 hours and transfecting with a knockdown of neuronal miR-146a-5p. We assessed the expression levels of mmu-miR-146a-5p and *NOTCH1* using RT-qPCR. The results of the RT-qPCR analysis demonstrated a significant decrease in mmu-miR-146a-5p expression ($t_4 = 8.522$, $p = 0.001$) and a significant increase in *NOTCH1* expression ($t_4 = 5.346$, $p = 0.006$) in the miR-146a-5p inhibitor group, compared with the miR-NC inhibitor group (Figure 12A). In addition, the results of the CCK-8 assay and LDH release experiment showed that the neuronal activity of the miR-146a-5p inhibitor group was significantly increased ($t_4 = 5.153$, $p = 0.007$; Figure 12B) and cell damage was reduced ($t_4 = 3.972$, $p = 0.02$; Figure 12C). Altogether, exosomal miR-146a-5p affected cortical pyramidal neuron activity and synaptic function in mice by inhibiting *NOTCH1* signalling.

Discussion

We analyzed SRA transcriptome sequencing data from the prefrontal cortex tissue of mice with schizophrenia. The differentially expressed genes were mainly enriched in synaptic regulation–related functions and pathways. Therefore, it can be hypothesized that the onset of schizophrenia may be related to the synaptic activity of pyramidal neurons in the lissencephalic gyrus. Meanwhile, it has been demonstrated in the literature that problems in neural development lead to abnormal functions of synaptic transmission and plasticity, which cause schizophrenia.[41] Synaptic activity can increase neuronal resistance to harmful conditions.[42] We concluded that plasma exosomal miR-146a-5p may inhibit *NOTCH1*-mediated synaptic activity of cortical pyramidal neurons through targeting and regulation of *NOTCH1*, which in turn promotes the onset and development of schizophrenia in mice (Figure 13). These findings highlight the important role of synapses in schizophrenia. Synaptic regulatory pathways can be explored to better understand the pathogenesis of schizophrenia.

To further elucidate the pathogenesis of schizophrenia, we retrieved the schizophrenia-related data set from mice in the GEO database and performed KEGG enrichment analysis.[43] Results suggested that genes associated with schizophrenia may be associated with neuronal degeneration.[44] Elsewhere, dendritic spine density and mean cell volume of pyramidal neurons were observed to be reduced in the cerebral cortex of patients with schizophrenia.[45] Considering these results, we hypothesize that the pathogenesis of schizophrenia may be controlled by molecular mechanisms regulating the expression of genes associated with the disease, which in turn leads to neuronal degeneration, affecting the neuronal synaptic activity and triggering schizophrenia. Our study further confirms the important role of neuronal synaptic activity in schizophrenia.

Previous research has reported that the functional impairments of cortical neurons in schizophrenia may, in part, be attributed to the dysregulation of gene network functions mediated by altered microRNA expression.[46] Moreover, studies have discovered that extracellular vesicles can exert certain effects on neuronal function by transferring small molecules into neurons.[20,21] Follow-up results on mouse prefrontal cortex tissue and plasma exosome microRNA sequencing showed that miR-146a-5p is a candidate target, highly expressed in both prefrontal cortex tissue and plasma

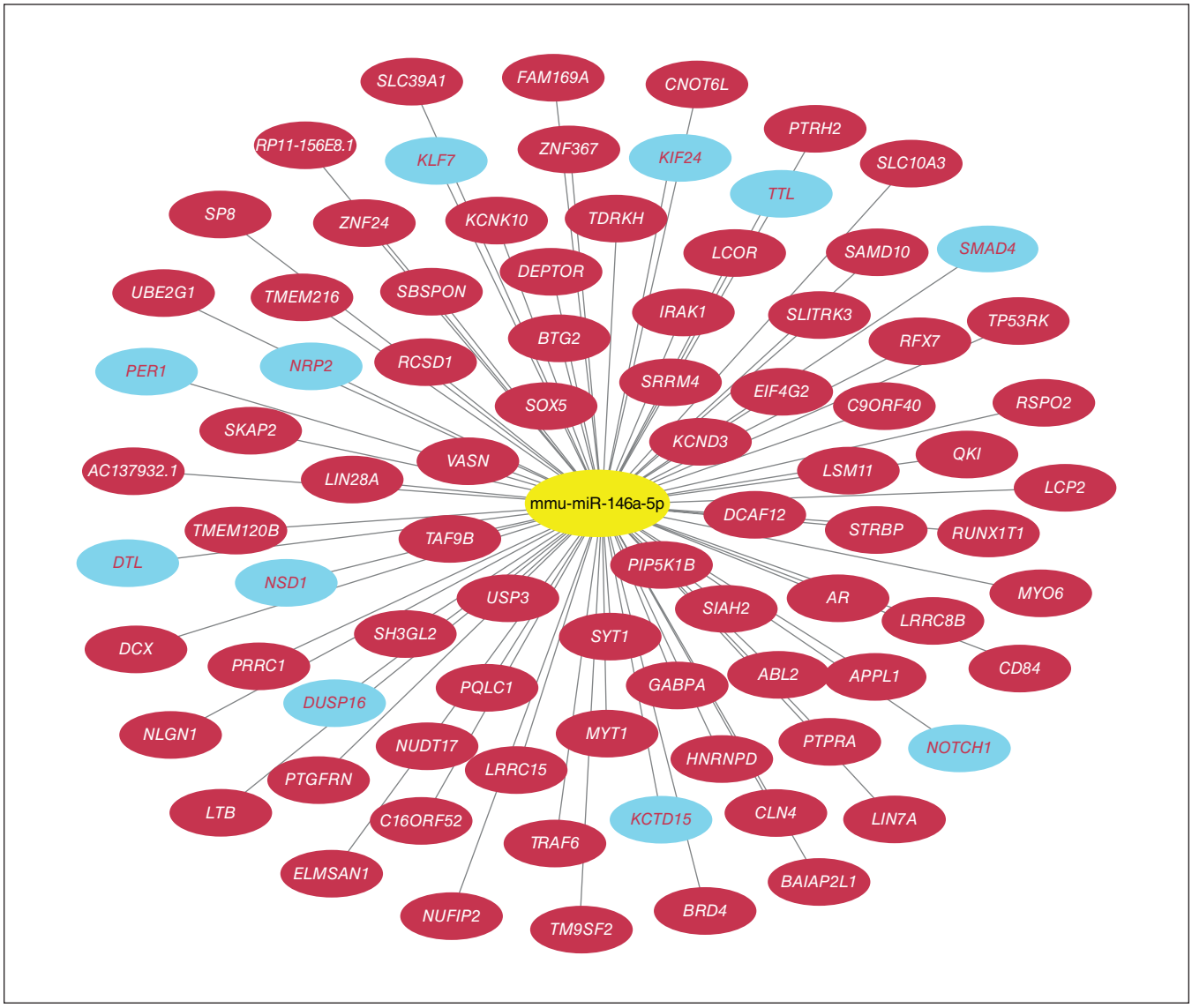

Figure 6: Cytoscape visualization of the microRNA–target gene regulatory network, where yellow represents mmu-miR-146a-5p, red represents mmu-miR-146a-5p target genes retrieved from the TargetScan database, and blue represents the 11 mmu-miR-146a-5p target genes retrieved from the TargetScan database that were simultaneously differentially expressed in prefrontal cortex tissue of mice with schizophrenia (i.e., *NOTCH1*, *KLF7*, *KIF24*, *TTL*, *SMAD4*, *PER1*, *NRP2*, *DTL*, *NSD1*, *DUSP16*, and *KCTD15*).

exosomes.[47] Consistently, miR-146a-5p is highly expressed in neurodegenerative diseases, including Alzheimer disease and prion disease.[48,49] Notably, increased expression of miR-146a has been observed in peripheral blood mononuclear cells of patients with schizophrenia.[50] Moreover, microRNAs play essential roles in the central nervous system by regulating genes involved in neurodevelopment and synaptic plasticity. Dysregulation of these microRNAs can disrupt synaptic protein regulation and neuronal connectivity, potentially contributing to the cognitive deficits observed in schizophrenia. Specifically, miR-146a-5p's modulation of the Notch signalling pathway underscores its influence on neuroprotective and synaptic functions, offering insights into novel therapeutic targets for disorders of the central nervous system. In addition, upregulation of miR-146a-5p has been demonstrated in plasma exosomes from patients with early syphilis, and miR-146a-5p can be transmitted between cells via plasma exosomes.[51] This is consistent with our observation that plasma exosomes can transfer miR-146a-5p to pyramidal neurons of the lissencephalic gyrus, where it may target *NOTCH1* and inhibit synaptic activity mediated by the Notch signalling pathway, ultimately promoting the onset and progression of schizophrenia in mice.

According to a recent study, miR-146a-5p directly targets the 3′-untranslated region of *NOTCH1* and inhibits its expression in dental pulp stem cells; in addition, miR-146a-5p partially regulates the differentiation and proliferation of dental pulp stem cells by inhibiting the Notch signalling

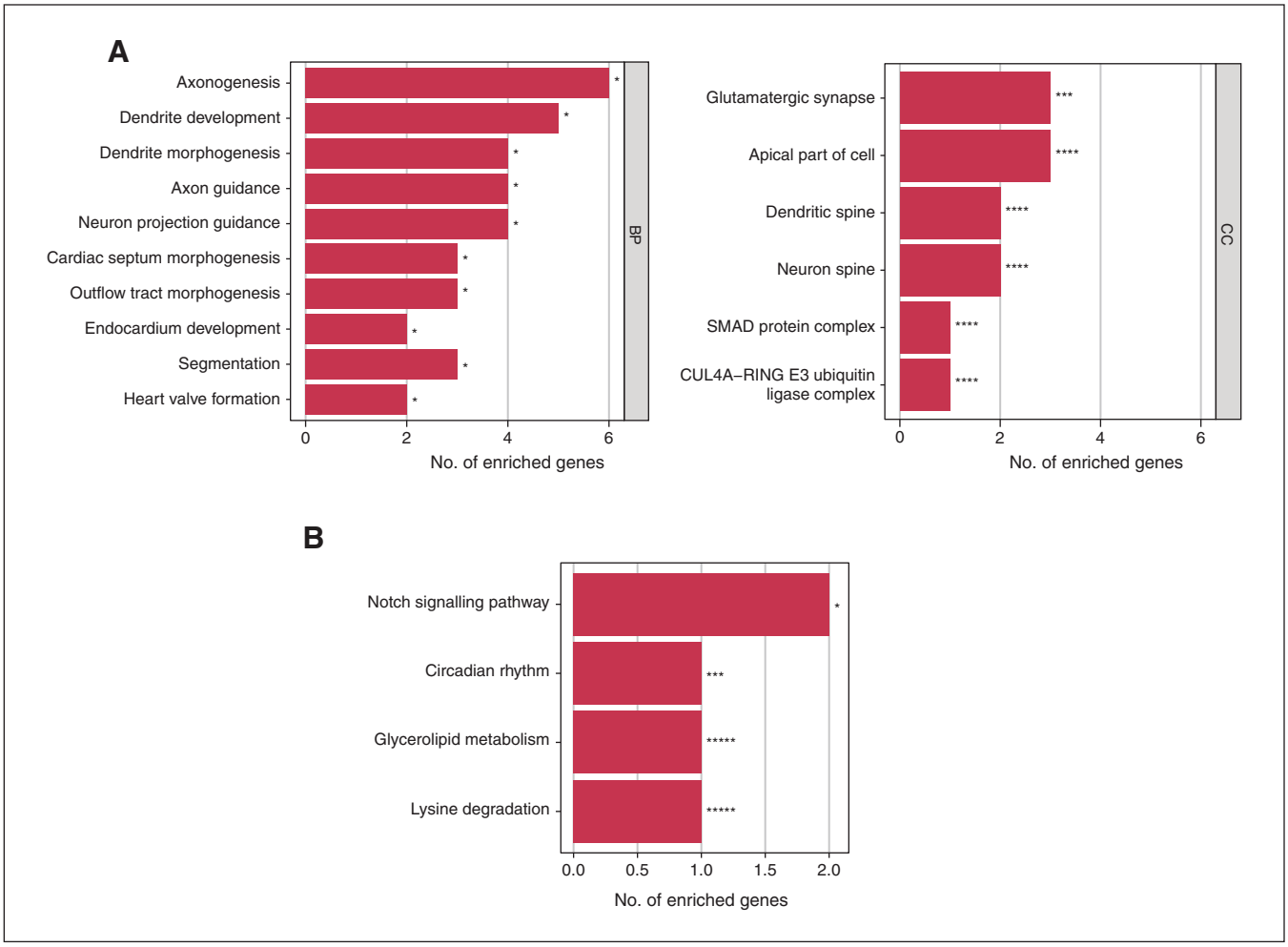

Figure 7: (A) Gene Ontology (GO) enrichment analysis of 11 target genes of mmu-miR-146a-5p (identified with GO name), indicating number of enriched genes and significance of difference between mice with schizophrenia and controls. (B) Kyoto Encyclopedia of Genes and Genomes (KEGG) enrichment analysis of 11 target genes of mmu-miR-146a-5p (identified with KEGG name), indicating number of enriched genes and significance of difference between mice with schizophrenia and controls. See Related Content tab for accessible version. BP = biological process, CC = cellular component. *$p < 0.01$; **$p < 0.02$; ***$p < 0.03$; ****$p < 0.04$; *****$p < 0.05$.

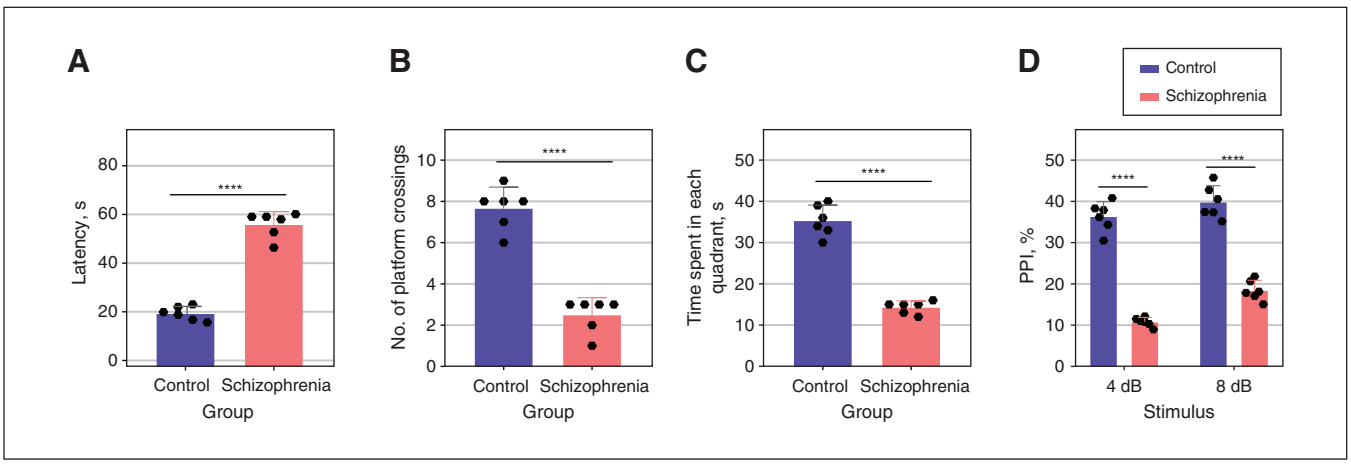

Figure 8: Validation of the schizophrenia mouse model and effects of plasma exosomal miR-146a-5p on cortical pyramidal neuron activity. (A) Latency to escape in mice. (B) Number of times mice crossed the original platform. (C) Time spent by mice in each quadrant. (D) Pre-pulse inhibition test to assess response inhibition. See Related Content tab for accessible version. ****$p < 0.0001$.

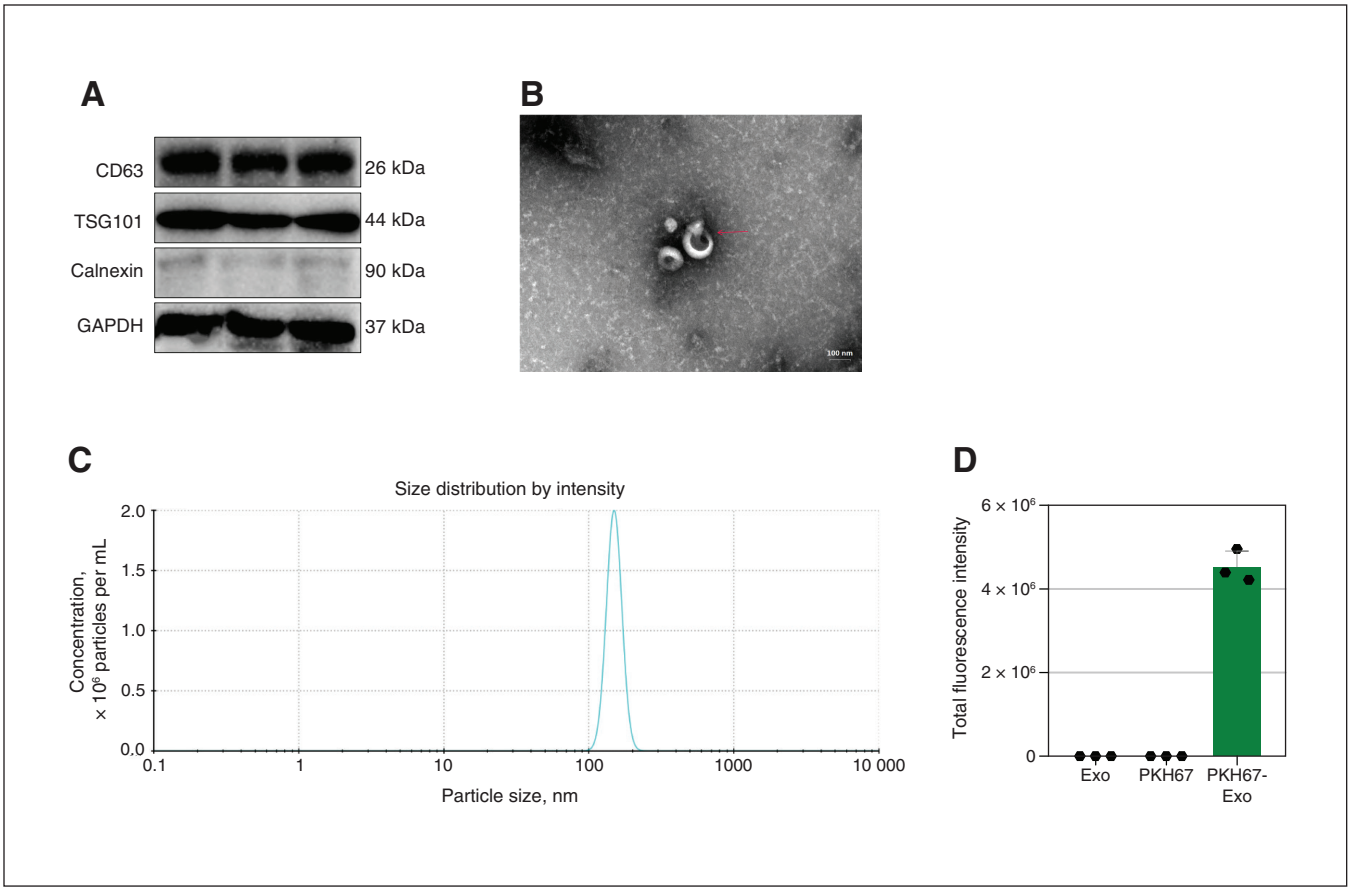

Figure 9: (A) The expression of exosome marker proteins (CD63, TSG101, calnexin, glyceraldehyde 3-phosphate dehydrogenase [GADPH]), detected by Western blot. (B) Exosome morphology was observed by transmission electron microscopy (40 000× magnification) after negative staining with phosphotungstic acid suspension. (C) Particle size distribution and particle concentration of plasma exosome, measured by nanoparticle tracer analyzer. (D) Immunofluorescence detected the uptake of PKH67-labelled exosomes by cortical neurons (Exo indicates unlabelled exosomes, PKH67 indicates pure dye, and PKH67-Exo indicates staining of labelled exosomes after co-culture with neurons).

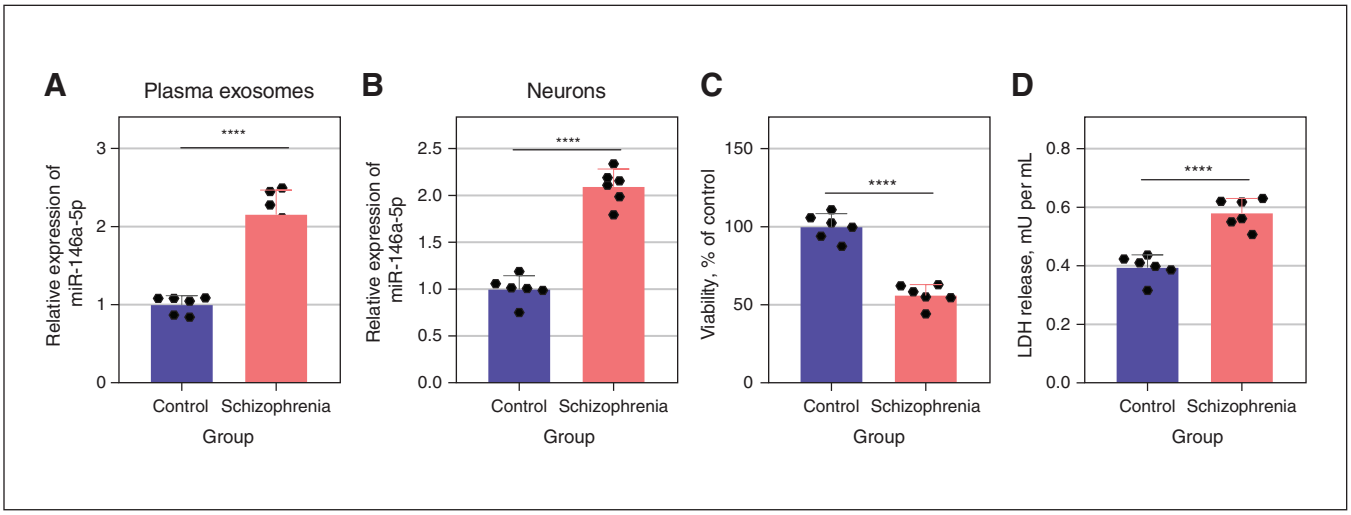

Figure 10: (A) Expression level of miR-146a-5p in plasma-derived extracellular vesicles, detected by reverse transcription quantitative polymerase chain reaction (RT-qPCR). (B) Expression of miR-146a-5p in neurons co-cultured with exosomes, detected by RT-qPCR. (C) Neuronal activity and (D) injury after co-culture, detected by cell counting and lactate dehydrogenase (LDH) release assay, respectively. See Related Content tab for accessible version. ****$p < 0.0001$.

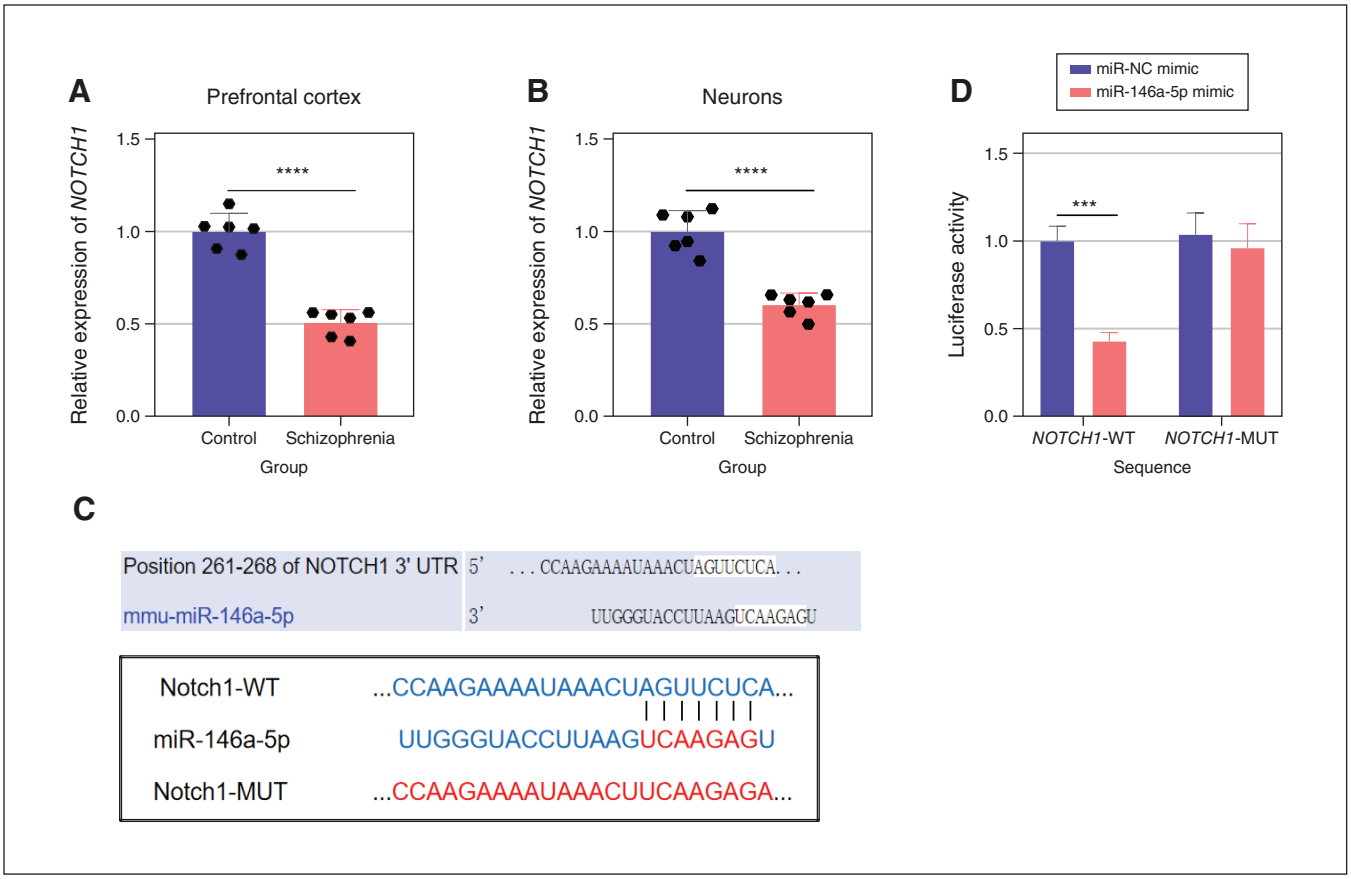

Figure 11: (A) Expression level of *NOTCH1* in prefrontal cortex tissue among mice with schizophrenia and controls, detected by reverse transcription quantitative polymerase chain reaction (RT-qPCR). (B) The expression of *NOTCH1* in neurons co-cultured with exosomes among mice with schizophrenia and controls, detected by RT-qPCR. (C) Prediction of miR-146a-5p binding sites to wild-type (*NOTCH1*-WT) or mutant (*NOTCH1*-MUT) *NOTCH1* sequences by TargetScan database. (D) Interaction between *NOTCH1* and miR-146a-5p mimic or miR-NC mimic, verified by dual-luciferase reporter gene assay. See Related Content tab for accessible version. UTR = untranslated region. ***$p < 0.001$; ****$p < 0.0001$.

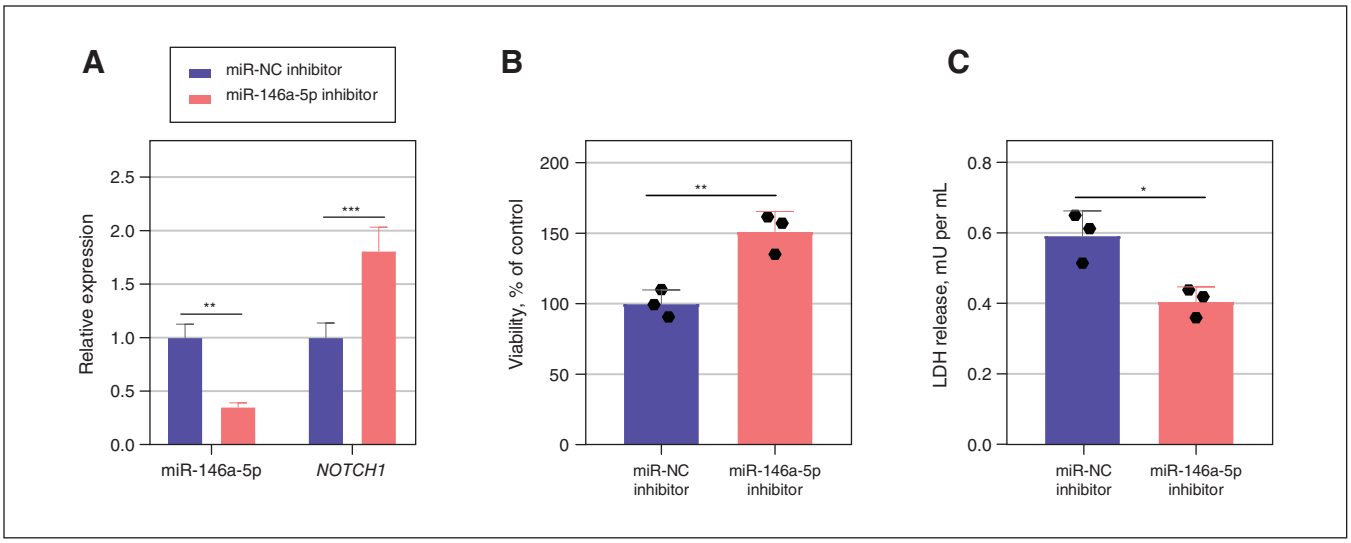

Figure 12: (A) Expression of miR-146a-5p and *NOTCH1*, evaluated using reverse transcription quantitative polymerase chain reaction, in neurons after co-cultivation with exosomes derived from mice with schizophrenia and subsequent knockdown of miR-146a-5p expression with miR-146a-5p inhibitor, compared with miR-NC inhibitor. (B) Neuronal activity and (C) injury after co-culture, detected by cell counting and lactate dehydrogenase (LDH) release assay, respectively. See Related Content tab for accessible version. *$p < 0.05$; **$p < 0.01$; ***$p < 0.001$.

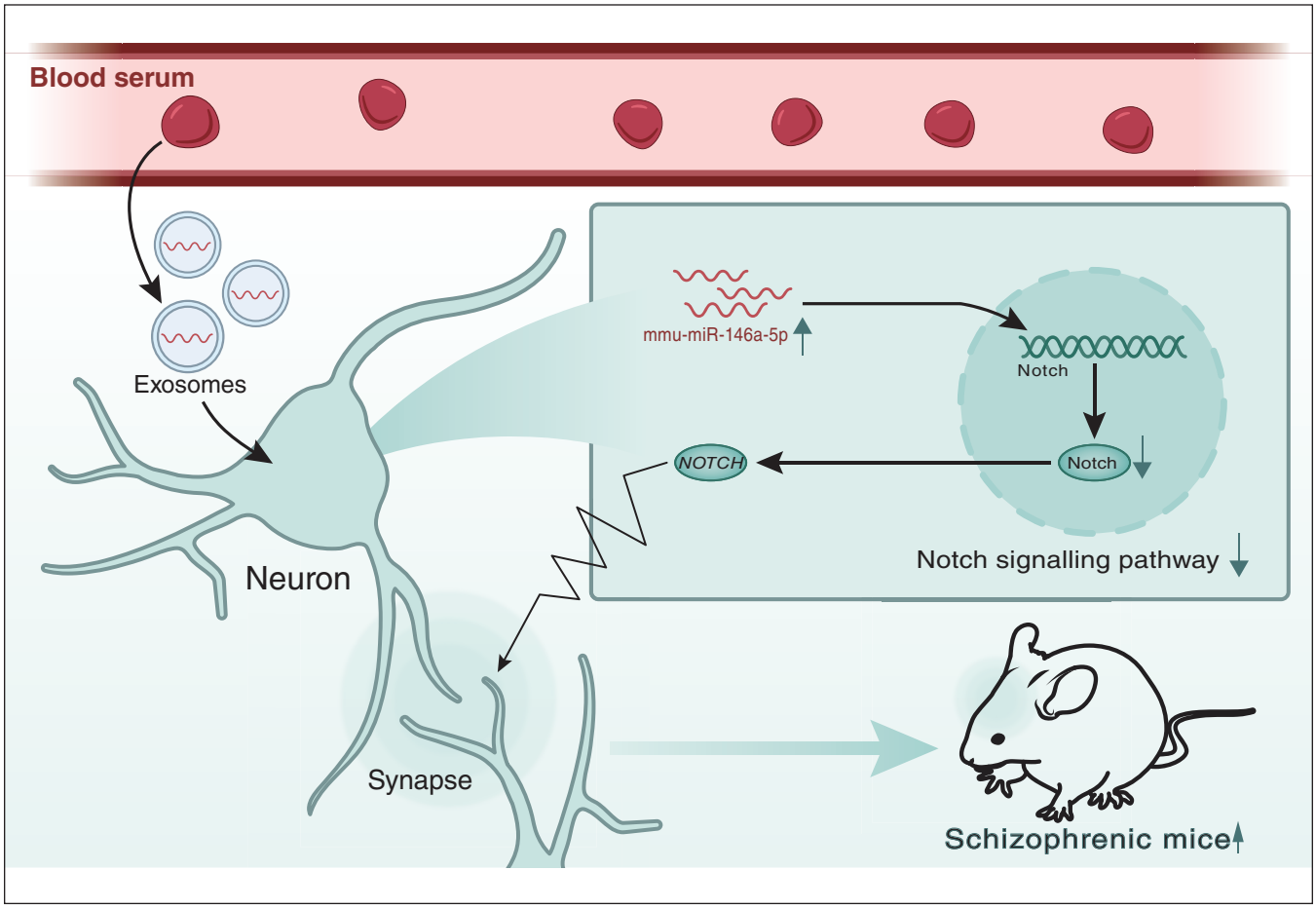

Figure 13: Schematic diagram of the molecular mechanism of plasma exosome mmu-miR-146a-5p expression in schizophrenia.

pathway.[52] Neurodevelopmental abnormalities are the strongest hypothesis regarding the etiology of schizophrenia, and neurodevelopmental processes are associated with many signalling pathways, including the Notch signalling pathway.[53] In previous studies, receptor-interacting protein (RIP) was found to play a role in mouse models of schizophrenia by upregulating Notch signalling pathway–related molecules (e.g., Notch1, Hes1, Hes) to improve cognitive impairment and restore cell proliferation in MK-801–treated mice.[54] In addition, Notch1 is present in synapses, and the Notch signalling pathway in neurons occurs in response to stimulation of synaptic activity; this pathway can be positively regulated by *ARC/ARG3.1*, a gene required for synaptic plasticity.[55] Previous studies identified the importance of the Notch signalling pathway and its capability in regulating synaptic transmission through the activation of neuroprotective genes associated with Alzheimer disease.[56] Meanwhile, miR-146a treatment of motor neurons resulted in the downregulation of extracellular matrix genes associated with perisynaptic neuronal accumulation nets and altered spontaneous electrical physiologic activity.[57] These data emphasize the important role of the miR-146a-5p–mediated Notch signalling pathway in synaptic activity.

Limitations

We did not provide direct evidence to support the conclusion that miR-146a-5p may inhibit Notch1 and synaptic plasticity mediated by Notch in mouse cortical pyramidal neurons. We intend to address this issue through further experiments in future studies. To better support this hypothesis, our future research directions include functional analysis, including conducting additional experiments involving plasma-derived exosomes, miR-146a-5p, and Notch1 treatment to investigate the impact of miR-146a-5p on *NOTCH1* expression and Notch-mediated synaptic plasticity. This will involve both in vitro and in vivo experiments to gain a more comprehensive understanding of the underlying mechanisms involved in this association. We will also search for additional biomarkers of synaptic plasticity and evaluate their relationship with miR-146a-5p and Notch1 to provide more direct evidence supporting our conclusions. We will further refine the animal model by combining plasma-derived exosomes, miR-146a-5p, and Notch1 to explore the reliability and applicability of the relevant mechanisms in a mouse model of schizophrenia.

Conclusion

Based on our results and a review of the literature, mmu-miR-146a-5p in plasma-derived exosomes may regulate expression of *NOTCH1* in cortical pyramidal neurons, thus inhibiting synaptic activity mediated by the Notch signalling pathway and, ultimately, promoting the occurrence and development of schizophrenia in mice. Although the evidence is robust, further validation is necessary at the cellular, animal, and clinical levels.

Affiliations: From the Departments of Academic Research, Qiqihar Medical University, Qiqihar, PR China (Z. Wang); the School of Basic Medical Sciences, Nanchang University, Nanchang, PR China (Hu); the Community Medicine Department, Faculty of Medicine, Lincoln University College, Malaysia (Alabed); the Department of Psychology, Qiqihar Medical University, Qiqihar, PR China (Wu, Cui, L. Sun, Z. Sun).

Competing interests: None declared.

Contributors: Zhichao Wang, Tong Wu, Houjia Hu, and Guangcheng Cui contributed to the conception and design of the work. All of the authors contributed to data acquisition, analysis, and interpretation. Zhichao Wang and Tong Wu drafted the manuscript. All of the authors revised it critically for important intellectual content, gave final approval of the version to be published, and agreed to be accountable for all aspects of the work.

Funding: This work was supported by the Natural Science Foundation of Heilongjiang Province (LH2020H130).

Data sharing: The data are available on request from the corresponding author.

References

1. Paul SM, Yohn SE, Popiolek M, et al. Muscarinic acetylcholine receptor agonists as novel treatments for schizophrenia. *Am J Psychiatry* 2022;179:611-27.
2. Trindade VC, Carneiro-Sampaio M, Bonfa E, et al. An update on the management of childhood-onset systemic lupus erythematosus. *Paediatr Drugs* 2021;23:331-47.
3. Förster K, Kanske P. Upregulating positive affect through compassion: psychological and physiological evidence. *Int J Psychophysiol* 2022;176:100-7.
4. Yang J, Kudulaiti N, Chen Z, et al. Within and beyond the visual cortex: brain tumors induce highly sensitive plasticity of visual processing in whole-brain neural functional networks. *Cereb Cortex* 2022;32:4422-35.
5. de Mendonça Filho EJ, Barth B, Bandeira DR, et al. Cognitive development and brain gray matter susceptibility to prenatal adversities: moderation by the prefrontal cortex brain-derived neurotrophic factor gene co-expression network. *Front Neurosci* 2021;15:744743.
6. Yeo XY, Tan LY, Chae WR, et al. Liver's influence on the brain through the action of bile acids. *Front Neurosci* 2023;17:1123967.
7. Colucci-D'Amato L, Speranza L, Volpicelli F. Neurotrophic factor BDNF, physiological functions and therapeutic potential in depression, neurodegeneration and brain cancer. *Int J Mol Sci* 2020;21:7777.
8. Mendell JR, Al-Zaidy SA, Rodino-Klapac LR, et al. Current clinical applications of in vivo gene therapy with AAVs. *Mol Ther* 2021;29:464-88.
9. Quinn PMJ, Moreira PI, Ambrósio AF, et al. PINK1/PARKIN signalling in neurodegeneration and neuroinflammation. *Acta Neuropathol Commun* 2020;8:189.
10. Kjeldsen EW, Nordestgaard LT, Frikke-Schmidt R. HDL cholesterol and non-cardiovascular disease: a narrative review. *Int J Mol Sci* 2021;22:4547.
11. Zoulikha M, Xiao Q, Boafo GF, et al. Pulmonary delivery of siRNA against acute lung injury/acute respiratory distress syndrome. *Acta Pharm Sin B* 2022;12:600-20.
12. Kahn RS, Sommer IE, Murray RM, et al. Schizophrenia. *Nat Rev Dis Primers* 2015;1:15067.
13. Volk DW, Lewis DA. Prefrontal cortical circuits in schizophrenia. *Curr Top Behav Neurosci* 2010;4:485-508.
14. Alvarez-Erviti L, Seow Y, Yin H, et al. Delivery of siRNA to the mouse brain by systemic injection of targeted exosomes. *Nat Biotechnol* 2011;29:341-5.
15. Izco M, Blesa J, Schleef M, et al. Systemic exosomal delivery of shRNA minicircles prevents parkinsonian pathology. *Mol Ther* 2019;27:2111-22.
16. Xu Y, Hu Y, Xu S, et al. Exosomal microRNAs as potential biomarkers and therapeutic agents for acute ischemic stroke: new expectations. *Front Neurol* 2022;12:747380.
17. Wei ZX, Xie GJ, Mao X, et al. Exosomes from patients with major depression cause depressive-like behaviors in mice with involvement of miR-139-5p-regulated neurogenesis. *Neuropsychopharmacology* 2020;45:1050-8.
18. Saeedi S, Nagy C, Ibrahim P, et al. Neuron-derived extracellular vesicles enriched from plasma show altered size and miRNA cargo as a function of antidepressant drug response. *Mol Psychiatry* 2021;26:7417-24.
19. Mori MA, Ludwig RG, Garcia-Martin R, et al. Extracellular miRNAs: from biomarkers to mediators of physiology and disease. *Cell Metab* 2019;30:656-73.
20. Zhang Y, Chopp M, Liu XS, et al. Exosomes derived from mesenchymal stromal cells promote axonal growth of cortical neurons. *Mol Neurobiol* 2017;54:2659-73.
21. Kong FL, Wang XP, Li YN, et al. The role of exosomes derived from cerebrospinal fluid of spinal cord injury in neuron proliferation in vitro. *Artif Cells Nanomed Biotechnol* 2018;46:200-5.
22. Zhou Y, Peng W, Wang J, et al. Plasma levels of IL-1Ra are associated with schizophrenia. *Psychiatry Clin Neurosci* 2019;73:109-15.
23. Ables JL, Breunig JJ, Eisch AJ, et al. Not(ch) just development: Notch signalling in the adult brain. *Nat Rev Neurosci* 2011;12:269-83.
24. Wei J, Hemmings GP. The *NOTCH4* locus is associated with susceptibility to schizophrenia. *Nat Genet* 2000;25:376-7.
25. Stefansson H, Ophoff RA, Steinberg S, et al. Common variants conferring risk of schizophrenia. *Nature* 2009;460:744-7.
26. Radtke F, Fasnacht N, Macdonald HR. Notch signaling in the immune system. *Immunity* 2010;32:14-27.
27. Butko E, Pouget C, Traver D. Complex regulation of HSC emergence by the Notch signaling pathway. *Dev Biol* 2016;409:129-38.
28. Quillard T, Charreau B. Impact of Notch signaling on inflammatory responses in cardiovascular disorders. *J Mol Sci* 2013;14:6863-88.
29. Shang Y, Smith S, Hu X. Role of Notch signaling in regulating innate immunity and inflammation in health and disease. *Protein Cell* 2016;7:159-74.
30. Bergink V, Gibney SM, Drexhage HA. Autoimmunity, inflammation, and psychosis: a search for peripheral markers. *Biol Psychiatry* 2014;75:324-31.
31. Zuo Y, Iemolo A, Montilla-Perez P, et al. Chronic adolescent exposure to cannabis in mice leads to sex-biased changes in gene expression networks across brain regions. *Neuropsychopharmacology* 2022;47:2071-80.
32. Liang JQ, Chen X, Cheng Y. Paeoniflorin rescued MK-801-induced schizophrenia-like behaviors in mice via oxidative stress pathway. *Front Nutr* 2022;9:870032.
33. Rodríguez G, Neugebauer NM, Yao KL, et al. 9-tetrahydrocannabinol (Δ9-THC) administration after neonatal exposure to phencyclidine potentiates schizophrenia-related behavioral phenotypes in mice. *Pharmacol Biochem Behav* 2017;159:6-11.
34. Baranyai T, Herczeg K, Onódi Z, et al. Isolation of exosomes from blood plasma: qualitative and quantitative comparison of ultracentrifugation and size exclusion chromatography methods. *PLoS One* 2015;10:e0145686.

35. Kulabukhova DG, Garaeva LA, Emelyanov AK, et al. [Plasma exosomes in inherited forms of parkinson's disease]. *Mol Biol (Mosk)* 2021;55:338-45.
36. Zhou L, Chang J, Zhou M, et al. [Cypermethrin induces cell injury in primary cortical neurons of C57BL/6 mice by inhibiting Nrf2/ARE signaling pathway]. *Nan Fang Yi Ke Da Xue Xue Bao* 2019;39:1469-75.
37. Liu W, Rong Y, Wang J, et al. Exosome-shuttled miR-216a-5p from hypoxic preconditioned mesenchymal stem cells repair traumatic spinal cord injury by shifting microglial M1/M2 polarization. *J Neuroinflammation* 2020;17:47.
38. Zhu D, Zhang J, Wu J, et al. Paliperidone protects SH-SY5Y cells against MK-801-induced neuronal damage through inhibition of Ca^{2+} influx and regulation of SIRT1/miR-134 signal pathway. *Mol Neurobiol* 2016;53:2498-509.
39. Tong L, Wang Y, Ao Y, et al. CREB1 induced lncRNA HAS2-AS1 promotes epithelial ovarian cancer proliferation and invasion via the miR-466/RUNX2 axis. *Biomed Pharmacother* 2019;115:108891.
40. Zou S, Wang C, Cui Z, et al. β-Elemene induces apoptosis of human rheumatoid arthritis fibroblast-like synoviocytes via reactive oxygen species-dependent activation of p38 mitogen-activated protein kinase. *Pharmacol Rep* 2016;68:7-11.
41. Chen P, Jing H, Xiong M, et al. Spine impairment in mice high-expressing neuregulin 1 due to LIMK1 activation. *Cell Death Dis* 2021;12:403.
42. Kim YS, Choi J, Yoon BE. Neuron-glia interactions in neurodevelopmental disorders. *Cells* 2020;9:2176.
43. Li Z, Li X, Jin M, et al. Identification of potential biomarkers and their correlation with immune infiltration cells in schizophrenia using combinative bioinformatics strategy. *Psychiatry Res* 2022;314:114658.
44. Namme JN, Bepari AK, Takebayashi H. Cofilin signaling in the CNS physiology and neurodegeneration. *Int J Mol Sci* 2021;22:10727.
45. Jossin Y. Reelin functions, mechanisms of action and signaling pathways during brain development and maturation. *Biomolecules* 2020;10:964.
46. Pietersen CY, Mauney SA, Kim SS, et al. Molecular profiles of pyramidal neurons in the superior temporal cortex in schizophrenia. *J Neurogenet* 2014;28:53-69.
47. Fan C, Li Y, Lan T, et al. Microglia secrete miR-146a-5p-containing exosomes to regulate neurogenesis in depression. *Mol Ther* 2022;30:1300-14.
48. Lei B, Liu J, Yao Z, et al. NF-κB-induced upregulation of miR-146a-5p promoted hippocampal neuronal oxidative stress and pyroptosis via TIGAR in a model of alzheimer's disease. *Front Cell Neurosci* 2021;15:653881.
49. Jia L, Zhu M, Yang J, et al. Prediction of P-tau/Aβ42 in the cerebrospinal fluid with blood microRNAs in Alzheimer's disease. *BMC Med* 2021;19:264.
50. Tseng CC, Wang SC, Yang YC, et al. Aberrant histone modification of TNFAIP3, TLR4, TNIP2, miR-146a, and miR-155 in major depressive disorder. *Mol Neurobiol* 2023;60:4753-60.
51. Hu W, Xu B, Zhang J, et al. Exosomal miR-146a-5p from *Treponema pallidum*-stimulated macrophages reduces endothelial cells permeability and monocyte transendothelial migration by targeting JAM-C. *Exp Cell Res* 2020;388:111823.
52. Chen X, Su C, Wei Q, et al. Exosomes derived from human umbilical cord mesenchymal stem cells alleviate diffuse alveolar hemorrhage associated with systemic lupus erythematosus in mice by promoting M2 macrophage polarization via the microRNA-146a-5p/NOTCH1 axis. *Immunol Invest* 2022;51:1975-93.
53. Casas BS, Arancibia-Altamirano D, Acevedo-La Rosa F, et al. It takes two to tango: widening our understanding of the onset of schizophrenia from a neuro-angiogenic perspective. *Front Cell Dev Biol* 2022;10:946706.
54. Grilli G, Hermida-Prado F, Álvarez-Fernández M, et al. Impact of Notch signaling on the prognosis of patients with head and neck squamous cell carcinoma. *Oral Oncol* 2020;110:105003.
55. Tyagi A, Sharma AK, Damodaran C. A review on Notch signaling and colorectal cancer. *Cells* 2020;9:1549.
56. Perna A, Marathe S, Dreos R, et al. Revealing NOTCH-dependencies in synaptic targets associated with Alzheimer's disease. *Mol Cell Neurosci* 2021;115:103657.
57. Chen Y, Chen J, Chen Y, et al. miR-146a/KLF4 axis in epileptic mice: a novel regulator of synaptic plasticity involving STAT3 signaling. *Brain Res* 2022;1790:147988.